 doi:10.20944/preprints201705.0029.v1

Causal Pathways for Temperature Predictability from Snow Depth

ERIK W. KOLSTAD

Uni Research Climate, Bjerknes Centre for Climate Research, Bergen, Norway[*]

ABSTRACT

Subseasonal-to-seasonal (S2S) weather forecasting has improved in recent years, thanks partly to better representation of physical variables in models. For instance, realistic initializations of snow and soil moisture in models yield enhanced predictability on S2S time scales. Snow depth and soil moisture also mediate month-to-month persistence of near-surface air temperature. Here the role of snow depth as predictor of temperature one month ahead in the Northern Hemisphere is probed via two causal pathways. Through the first pathway, snow depth anomalies in month 1 cause snow depth anomalies in month 2, which then cause temperature anomalies in month 2. This pathway represents the snow–albedo feedback, as well as cooling due to insulation, emissivity and heat loss. It is active from fall to summer, and its effect peaks in March/April in the midlatitudes and in May/June at high latitudes. A complementary second pathway, where snow depth anomalies in month 1 cause soil moisture anomalies in month 2, which then cause temperature anomalies in month 2 through soil moisture–temperature feedbacks, is only active in spring and summer. Its effect peaks later in the warm season than the effect of the first pathway. Geographically, snow depth mediates north of, and soil moisture south of, the areas with the highest temperature predictability from snow depth. These results indicate that the two pathways describe complementary physical mechanisms. The first pathway embodies month-to-month persistence of snow depth, and the second pathway represents melting of snow from one month to the next.

Keywords

soil moisture; snow cover; snow depth; seasonal prediction; land–surface feedbacks; cryosphere

1. Introduction

Recently, dynamical subseasonal-to-seasonal (S2S) forecast model systems have achieved impressive skill (Saha et al., 2013; Domeisen et al., 2014; Scaife et al., 2014; Dunstone et al., 2016; Weisheimer et al., 2017). One reason is improvements of the representations of initial states. For instance, realistic initialization of snow enhances the forecast skill on S2S time scales (Schlosser and Mocko, 2003; Peings et al., 2011; Jeong et al., 2012; Orsolini et al., 2013; Lin et al., 2016). Similar results have been obtained by initializing soil moisture (Dirmeyer, 2000; Douville, 2003; Conil et al., 2009; Koster et al., 2010; Koster et al., 2011; van den Hurk et al., 2012; Kumar et al., 2014), as well as both snow and soil moisture (Douville, 2010; Prodhomme et al., 2016; Thomas et al., 2016).

Here, the focus is on the role of snow depth as empirical predictor of near-surface air temperature (hereafter just 'temperature') anomalies one month ahead. It is well-known that snow depth and snow cover can influence temperature on S2S time scales. For instance, Dutra et al. (2011) obtained model results indicating that more than half of the interannual temperature variability could be explained by snow cover and snow depth in snow-covered regions. Both on regional scales and over large geographical distances, dynamical feedbacks between snow and the atmospheric circulation have been identified (e.g., Foster et al., 1983; Cohen and Entekhabi, 1999; Cohen et al., 2007; Fletcher et al., 2009; Orsolini and Kvamstø, 2009; Sobolowski et al., 2010).

Using methods from statistical mediation analysis (Baron and Kenny, 1986; MacKinnon et al., 2007), two causal pathways are investigated to identify the mechanisms that mediate the temperature predictability from snow depth. The same framework was recently used by Kolstad et al. (2017) to quantify the roles of snow depth, soil moisture and soil temperature in mediating month-to-month temperature persistence.

In Pathway A, snow depth in month 1 predicts temperature in month 2 through snow depth as the mediating variable in month 2. Pathway A is therefore associated with persistence of snow, and is related to well-known instantaneous interplays between snow on temperature. The snow–albedo feedback (Thackeray and Fletcher,

[*] Corresponding author address: Dr. Erik W. Kolstad, Uni Research Climate, Allégaten 70, 5007 Bergen, Norway. E-mail: erik.kolstad@uni.no

Preprints (www.preprints.org) | NOT PEER-REVIEWED | Posted: 3 May 2017 doi:10.20944/preprints201705.0029.v1

2016) arises because snow has high albedo and reflects most of the incoming solar radiation, which leads to lower maximum air temperatures (Dewey, 1977). This impedes melting and therefore maintains the high surface albedo. A related feedback is associated with the insulating effect of snow (Zhang, 2005); deep snow yields lower air temperatures because heat fluxes from below are obstructed, which again prohibits melting. The high emissivity and large heat loss of snow leads to lower minimum temperatures (Dewey, 1977). Many empirical studies (Wagner, 1973; Walsh et al., 1982; Namias, 1985; Leathers and Robinson, 1993; Bednorz, 2004; Mote, 2008) and dynamical model experiments (e.g. Cohen and Rind, 1991; Yasunari et al., 1991; Vavrus, 2007) describe the local cooling effect of snow.

In Pathway B, soil moisture as the mediating variable in month 2. This means that Pathway B is associated with melting, i.e. the opposite of snow persistence. In spring, positive snow depth anomalies in one month can lead to positive soil moisture anomalies in subsequent months if the snow melts, as suggested by Walsh et al. (1985). Wet soils are conducive to cold temperature anomalies due to soil moisture–temperature feedback mechanisms (Seneviratne et al., 2010). Conversely, negative snow depth anomalies can lead to future dry soil anomalies (due to lack of melting), which again lead to warm temperature anomalies. These relationships between snow depth anomalies and subsequent soil moisture anomalies have been explored in numerous studies (e.g., Shinoda, 2001; Matsumura and Yamazaki, 2012; Potopová et al., 2016).

2. Data and Methods

a. Data sources

The analysis is based on interannual time series of monthly mean 2-meter temperature, snow depth, and (volumetric) soil moisture in the surface layer (0–10 cm). To account for enhanced autocorrelations due to long-term trends, each time series was detrended (with negligible impact on the results).

The two main data sources are the NOAA-CIRES Twentieth Century Reanalysis (Compo et al., 2011), version 2c (20CR henceforth), and the ECMWF's ERA-20C reanalysis (Poli et al., 2016). The 20CR covers the period 1850–2014, but only the period 1900–2010 was used, because it overlaps with the ERA-20C period. Only a minimum of surface variables is assimilated in 20CR and ERA-20C. This means that their temperature, snow, and soil moisture fields are simulated, and may differ from observations. Two modern-era reanalyses–ERA-Interim/Land reanalysis (Balsamo et al., 2015) and MERRA-2, the updated version of MERRA (Rienecker et al., 2011)—are used here as reference data sets in Section 3.1. Note that we did not use MERRA-Land (Reichle et al., 2011), as the main improvements of MERRA-Land relative to MERRA were carried into the higher-resolution MERRA-2, and "MERRA-2 land hydrology estimates are better than those of MERRA-Land" (Reichle et al., 2017).

How do the two twentieth century reanalyses perform? Zampieri et al. (2016) found that 20CR and ERA-20C reproduced a heat wave index reasonably well compared to satellite-era reanalyses. The variability of daily soil moisture in 20CR was contrasted with other reanalyses and observational networks by Dirmeyer et al. (2016), and was found to have a consistent negative bias. ERA-Interim/Land had an average positive bias of similar magnitude. ERA-20C was not evaluated. As for snow, the onset of autumnal snowfall in Eurasia in 20CR was found by Peings et al. (2013) to correspond well with observations. The snow depth in both reanalyses was evaluated by Wegmann et al. (2016), using in-situ observations from Russian stations as reference. They found that ERA-20C had lower snow depths than 20CR at the start of the 20th century, yielding a positive trend over the century in ERA-20C. No such trend was found in 20CR. In the satellite era, the geographical pattern of snow depths was found to correspond reasonably well with observations, except that 20CR was overestimated the snow depth somewhat, while ERA-20C had lower snow depths in Northern Siberia.

It is beyond the scope of this paper to perform a full evaluation of the reanalyses. However, the interannual mean and standard deviation of snow depth and soil moisture in the four reanalyses are briefly investigated in Section 3.1.

b. Mediation analysis

The causal pathways presented earlier can be quantified using statistical mediation analysis. The *predictor* in month 1 is snow depth, and can be denoted as P_1. The predictand in month 2 is temperature, written as T_2. The *mediated effect* of P_1 on T_2 is mediated by a *mediator* (snow depth or soil moisture) in month 2, denoted as M_2. The pathways can be written as a causal chain (Pearl et al., 2016):

$$P_1 \rightarrow M_2 \rightarrow T_2. \quad (1)$$

Preprints (www.preprints.org) | NOT PEER-REVIEWED | Posted: 3 May 2017 doi:10.20944/preprints201705.0029.v1

A causal chain illustrates a scenario where P_1 has an effect on T_2, meaning that the two variables are significantly correlated. However, P_1 also has an effect on M_2, and M_2 has an effect on T_2. If the causal chain describes *full mediation* (Baron and Kenny, 1986), T_2 becomes *conditionally independent* of P_1 given M_2. This means that the entire effect of P_1 on T_2 is mediated by M_2. If just some of the effect of P_1 on T_2 is mediated by M_2, the causal chain describes partial mediation.

To formally check the nature of the mediation, three regressions, corresponding to Eqs. (1)–(3) in Fritz and MacKinnon (2007), are defined:

$$\hat{T}_2 = \tau P_1 + \zeta_1, \quad (2)$$

$$\hat{T}_2 = \tau' P_1 + \beta M_2 + \zeta_2, \quad (3)$$

$$\hat{M}_2 = \alpha P_1 + \zeta_3, \quad (4)$$

$\hat{T}_2$ in Eq. (2) is the predicted temperature in month 2, predicted by the predictor in month 1 (P_1). The total effect of P_1 on T_2 is the regression coefficient τ, and ζ_1 is the intercept. In Eq. (3), the mediator in month 2 (M_2) is a regressor in addition to P_1. The corresponding regression coefficients are β and τ', and ζ_2 is the intercept. intercept. β is also known as the effect of M_2 on T_2 controlled for P_1. In Eq. (4), M_2 is predicted by P_1. The regression coefficient α is the total effect of P_1 on M_2, and ζ_3 is the intercept.

The mediated effect of P_1 on T_2 through M_2 is the product $\alpha\beta$. Because the Greek letter μ is the equivalent equivalent of M (for 'mediated effect'), this product is hereafter referred to as $\mu \stackrel{\text{def}}{=} \alpha\beta$. If standardized anomalies are used, μ represents the predicted standardized temperature anomaly in month 2 after a +1 standard deviation snow depth or soil moisture anomaly in month 1, through mediation by snow depth or soil moisture anomalies in month 2. Another benefit of using standardized anomalies is that the total effects τ and α are then linear correlation coefficients.

As mentioned, the causal framework allows both full and partial mediation. Four 'steps' must be satisfied for full mediation (Fritz and MacKinnon, 2007):

1. The total effect of P_1 on T_2, i.e. τ in Eq. (2), must be significant.
2. The total effect of P_1 on M_2, i.e. α in Eq. (4), must be significant.
3. The effect of M_2 on T_2 controlled for P_1, i.e. β in Eq. (3), must be significant.
4. The effect of P_1 on T_2 controlled for M_2, i.e. τ' in Eq. (3), must be nonsignificant.

For partial mediation, Step 4 is less strict and is only that $|\tau'| < |\tau|$. In other words, T_2 does not become conditionally independent of P_1 if M_2 is included in the regression, but the effect of P_1 on T_2 controlled for M_2 is less than the total effect of P_1 on T_2. Partial mediation is considered in the present study.

3. Results

a. Snow depth and soil moisture in the reanalyses

In Fig. 1, two metrics of snow depth—the long-term mean and the interannual standard deviation—are shown for the four reanalyses, area-averaged in three latitude belts. Some locations (probably glaciers) at high latitudes have very high snow depths in ERA-Interim/Land and ERA-20C, such as in Iceland. To prevent these high values from unduly influencing the areal means, the snow depth for all locations with mean values of more than three meters is set to three meters. No changes are done when computing the standard deviation. Note that in the context of this study, the variability is more important than the mean values, as standardized anomalies are used in Eqs. (2–4).

Noting the narrow ranges of the y-axes for the low latitudes in Fig. 1a–b, the differences between the reanalyses are practically negligible. In the midlatitudes (Fig. 1c–d), the only notable difference is that 20CR has the most snow and the strongest variability in winter and spring. At high latitudes, however, differences emerge. Fig. 1e shows that ERA-Interim/Land and ERA-20C have the deepest average snow in summer, but this is mainly due to the locations with more than three meters of snow. In winter and spring, the average snow depth in 20CR is slightly higher than in the other reanalyses. The average standard deviation of snow depth (Fig. 1f) is comparable across the reanalyses except for the high values in ERA-Interim/Land in December.

It is not feasible to show maps of the snow depth metrics for each month and each data set, but animated maps are shown in the Supplemental Material. Just one example is shown here. Inspired by the discrepancy between ERA-Interim/Land and the other data sets for the area-averaged standard deviation of snow depth at high latitudes

Preprints (www.preprints.org) | NOT PEER-REVIEWED | Posted: 3 May 2017 doi:10.20944/preprints201705.0029.v1

in December (see Fig. 1f), values for each grid point north of about 30°N in that month are shown in Fig. 2. The geographical distributions of the variability are quite similar across the models. For instance, each model has a local maximum at the Central Siberian Plateau, but the values are higher in ERA-Interim/Land than in the other models. All the models also have local maxima near the coasts of northwestern and northeastern North America, and northeastern Eurasia.

The area-averaged mean soil moisture at low latitudes is comparable in ERA-Interim/Land, ERA-20C, and MERRA-2, but the mean values are higher in 20CR (Fig. 3a). The standard deviation is similar in all the data sets (Fig. 3b). In the midlatitudes, the mean soil moisture is higher in 20CR than in the other data sets in winter (Fig. 3c). In ERA-Interim/Land and ERA-20C, some subarctic locations south of 60°N in North America have high values throughout the year. This results in consistently higher average values in these data sets than in MERRA-2. The interannual variability (Fig. 3d) is substantially higher in 20CR than in the other products from fall to spring. In summer, the variability is higher in ERA-Interim/Land and ERA-20C. These patterns are, in the main, repeated at high latitudes (Fig. 3e–f), with even larger differences between the variability in ERA-Interim/Land and ERA-20C compared to MERRA-2 and 20CR in summer.

Animated maps of the soil moisture metrics are found in the Supplemental Material, but one example is given here. As will be shown later, June is an important month for soil moisture mediation at high latitudes. In this month, the variability is on the rise in ERA-Interim/Land and ERA-20C, and still high in 20CR (see Fig. 3f). In Fig. 4, the standard deviation of soil moisture in June is shown. A belt with high values in 20CR (Fig. 4d) has moved gradually northwards in the course of the preceding months, following the snowline. In ERA-Interim/Land (Fig. 4a) and ERA-20C (Fig. 4b), the standard deviation at high latitudes is still lower than in 20CR, but one month later the geographical distributions in the ERA products are similar to the one in 20CR in June (not shown). In MERRA-2 (Fig. 4a), the variability at high latitudes is low throughout the summer, unlike in the other data sets.

In summary, it is difficult to judge whether any of the data sets is 'better' than the others. The strategy used in the remaining analysis is to use both 20CR and ERA-20C, as these reanalyses, while both imperfect in their individual ways, provide the longest time series and therefore yield more statistical robustness than the modern-era reanalyses.

b. Temperature predictability and its pathways

As an indicator of the overall predictability, area-averaged values of τ in Eq. (2)—the total effect of snow depth on temperature—are shown as orange bars in Fig. 5. The area-averaging operation is symbolized by brackets, so that this quantity is written $[\tau]$. When averaging, τ is set to zero for grid points with nonsignificant correlation at the 5 percent level. To avoid spurious values for grid points that rarely have snow, τ is also set to zero when the long-term median of the snow depth for a grid point is less than 1 cm.

At low latitudes (Fig. 5a–b), snow depth is not, on average, a particularly useful predictor of temperature. The $[\tau]$ values never exceed 0.2 in absolute terms, indicating that a maximum of less than 5 percent of the temperature in month 2 is explained by snow depth fluctuations in month 1, although some isolated high-altitude locations have substantially more negative τ values than the area-average. There is general agreement between the reanalyses. The blue bars, which show the area-averaged mediated effect through Pathway A ($[\mu]_A$), indicate that snow depth in month 2 is the dominant mediator in winter. The area-averaged mediated effect of soil moisture through Pathway B ($[\mu]_B$) has negative values mainly in spring. Note that the $[\mu]_A$ is slightly lower than $[\tau]$ in some month pairs. This means that there may be other, canceling mechanisms not considered here at play.

In the midlatitudes (Fig. 5c–d), $[\tau]$ is negative in October/November, probably because snow starts to fall in some locations. The dominance of $[\mu]_A$ over $[\mu]_B$ indicates that wintertime predictability is mainly mediated through Pathway A. The most negative $[\tau]$ values are found in spring, with gradually decreasing $[\mu]_B$ values. Qualitatively, the agreement between the two reanalyses is strong, although the total and mediated effects are larger in 20CR than in ERA-20C. The relative roles of the two pathways follow the same annual cycles. Pathway B dominates in April/May and May/June, and Pathway A is the leading causal chain from October/November to March/April.

At high latitudes (Fig. 5e–f), both reanalyses have nonzero $[\tau]$ values in fall (mediated through Pathway A). Although not shown, this effect is limited to the boundaries between the subartic and Tundra climate zones (Peel et al., 2007). The most negative $[\tau]$ values occur in spring, with peaks in May/June in both reanalyses. In 20CR, the peak absolute value is below −0.4, indicating that, on average, 15–20 percent of the temperature variability in June is explained by snow depth fluctuations in May. In ERA-20C, $[\mu]_A$ is closer to $[\tau]$ than $[\mu]_B$ until May/June. In 20CR, $[\mu]_B$ has the closest values to $[\tau]$ in May/June, and this is the case for both reanalyses in June/July. As

Preprints (www.preprints.org) | NOT PEER-REVIEWED | Posted: 3 May 2017 doi:10.20944/preprints201705.0029.v1

shown in Fig. 3f (and in the animations in the Supplemental Material), the soil moisture variability undergoes large changes in both ERA-20C and 20CR in June and July.

While the area-averaged toal and mediated effects shown in Fig. 5 provide a useful overview of the temperature predictability from snow depth, much of the regional detail contained in the data is lost. Therefore, maps of the total effect of snow depth on temperature, as well as the mediated effects through the two pathways, are now shown for the month pairs with the highest $[\tau]$ values in the mid- and high latitudes.

Fig. 6a–b show τ for each grid point in March/April, when $[\tau]$ peaks in the midlatitudes (see Fig. 5c–d). The reanalyses agree quite well on the geographical patterns. Broadly speaking, high τ values occur in the humid continental climate zones of both continents. In the midlatitudes, the highest mediated effect through Pathway A (μ_A; Fig. 6c–d) occurs slightly north of the regions with the highest τ values (Fig. 6a–b). The highest mediated effect through Pathway B (μ_B; Fig. 6e–f) occurs slightly south of those regions. This becomes clearer when the zonal means (excluding Greenland) of both τ and μ are computed. The latitude where the maximum values of the zonal means—denoted as $\bar{\tau}$, $\bar{\mu}_A$, and $\bar{\mu}_B$—are found are listed in Table 1 for the month pairs from late winter to early summer. In both data sets, the following inequalities are satisfied for all the month pairs: $\bar{\mu}_A \geq \bar{\tau} \geq \bar{\mu}_B$. Or in general terms: soil moisture mediation is most active to the south, and snow depth mediation to the north, of the areas with high temperature predictability from snow depth. A more trivial conclusion can also be inferred from the results in Table 1. For all three zonal mean quantities ($\bar{\tau}$, $\bar{\mu}_A$, and $\bar{\mu}_B$), the latitude where the maximum values occur increases with the time of the year, due to increasing insolation.

Maps for May/June are shown in Fig. 7. The agreement between the reanalyses is high in that the highest τ values are mainly found in the subarctic climate zones and in high-altitude areas (Fig. 7a–b). In Fig. 7c–f, μ_A and μ_B are shown. As is already known from Table 1, soil moisture mediates to the south of the regions with the highest τ values, and snow depth mediates to the north of those regions. For the May/June month pair, this is arguably easier to spot visually than it was for March/April in Fig. 6.

4. Discussion

It is already known from many previous studies that snow imparts predictability due to its persistence and its effects on temperature through physical mechanisms. What is new in this study is that the predictability of near-surface air temperature from snow depth has been quantified systematically in the extratropical Northern Hemisphere. Two causal pathways were investigated to shed light on why the temperature predictability associated with snow depth is highest during the melting season. Based on the results of the empirical analysis, the physical mechanisms that lead to the predictability are now discussed.

The first causal pathway—Pathway A—describes mediation by snow depth, and its average mediated effect ($[\mu] = [\alpha\beta]$) is negative (see Fig. 5). β in Eq. (3) is the lag-0 regression coefficient for snow depth anomalies on temperature. It can be assumed that β is negative. This means that α in Eq. (4), in this case the lag-1 autocorrelation of snow depth, must be positive (since $[\alpha\beta] < 0$). By implication, Pathway A represents persistence of snow depth from one month to the next (since $\alpha > 0$). Why is a mechanism related to persistence most active during the melting season? Probably because unusually strong (weak) persistence in the snow depth leads to unusually low (high) temperatures.

Soil moisture is the mediator in Pathway B, which also gives negative values for $[\alpha\beta]$ (see Fig. 5). Since β (the lag-0 regression coefficient for soil moisture anomalies on temperature) is usually negative due to soil moisture–temperature feedbacks (Seneviratne et al., 2010), α (the lag-1 correlation between snow depth and soil moisture) must be positive. This means that snow depth anomalies in month 1 are associated with soil moisture anomalies with the same sign in month 2. The physical mechanism for Pathway B, in other words, is that snow in month 1 has melted by month 2 if the snow depth anomalies in month 1 are positive. This yields positive soil moisture anomalies in month 2, which again give negative temperature anomalies through soil moisture–temperature feedbacks. Or conversely, lower-than-normal snow depths in month 1 lead to drier-than-normal soils and higher-than-normal temperatures in month 2.

Fig. 5 also showed that snow depth is the dominant mediator in winter in all three latitude belts used here, as the mediated effect $[\mu]_A$ is more negative, and therefore closer to the total effect $[\tau]$, than $[\mu]_B$. In all the latitude belts, $[\mu]_B$ takes over as the dominant term after the melting season has started. The zonal means of the total and mediated effects in Table 1 demonstrated that, from late winter to early summer, the mediated effect through Pathway A is largest north of the largest total effect, and the largest mediated effect through Pathway B

occurs south of the largest total effect. This geographical distribution, along with the phase differences of the annual marches of the two pathways shown in Fig. 5, indicate that Pathways A and B are complementary. Soil moisture mediation is associated with melting of snow and therefore occurs later in the warm season than snow depth mediation.

The study presented here illustrates how simple linear regressions can be powerful tools when applied to the framework of statistical mediation analysis. It is hoped that, together with other climate-related studies that have made use of causality analysis (e.g. Ebert-Uphoff and Deng, 2012; Runge et al., 2013; Kretschmer et al., 2016), this provides stimulus for future studies of complex, multivariate climatic interactions.

Acknowledgments

Funding for the author's work was given by the Research Council of Norway through the SNOWGLACE (grant 244166) and Seasonal Forecast Engine (grant 270733) projects. The 20CR data was downloaded from doi:10.5065/D6N877TW, and MERRA-2 from doi: 10.5067/8S35XF81C28F. The European Centre for Medium-Range Weather Forecasts (ECMWF) provided the ERA-20C and ERA-Interim/Land reanalyses, and the Global Modeling and Assimilation Office (GMAO) at NASA Goddard Space Flight Center provided the MERRA-2 data. Support for the Twentieth Century Reanalysis Project dataset is provided by the U.S. Department of Energy, Office of Science Innovative and Novel Computational Impact on Theory and Experiment (DOE INCITE) program, and Office of Biological and Environmental Research (BER), and by the National Oceanic and Atmospheric Administration (NOAA) Climate Program Office. The author wishes to thank Stefan Sobolowski and Yvan Orsolini for providing useful comments on an earlier version of the text.

References

Balsamo, G., and Coauthors, 2015: ERA-Interim/Land: a global land surface reanalysis data set. *Hydrology and Earth System Sciences*, **19**, 389-407.

Baron, R. M. and D. A. Kenny, 1986: The moderator–mediator variable distinction in social psychological research: Conceptual, strategic, and statistical considerations. *Journal of Personality and Social Psychology*, **51**, 1173–1182, doi:10.1037/0022-3514.51.6.1173.

Bednorz, E., 2004: Snow cover in eastern Europe in relation to temperature, precipitation and circulation. *Int. J. Climatol.*, **24**, 591-601, doi:10.1002/joc.1014.

Cohen, J. and D. Rind, 1991: The Effect of Snow Cover on the Climate. *J. Clim.*, **4**, 689-706, doi:10.1175/1520-0442(1991)004<0689:TEOSCO>2.0.CO;2.

Cohen, J. and D. Entekhabi, 1999: Eurasian snow cover variability and Northern Hemisphere climate predictability. *Geophys. Res. Lett.*, **26**, 345-348, doi:10.1029/1998gl900321.

Cohen, J., M. Barlow, P. J. Kushner, and K. Saito, 2007: Stratosphere–Troposphere Coupling and Links with Eurasian Land Surface Variability. *J. Clim.*, **20**, 5335-5343.

Compo, G. P., and Coauthors, 2011: The Twentieth Century Reanalysis Project. *Q. J. R. Meteorol. Soc.*, **137**, 1-28, doi:10.1002/qj.776.

Conil, S., H. Douville, and S. Tyteca, 2009: Contribution of realistic soil moisture initial conditions to boreal summer climate predictability. *Clim. Dyn.*, **32**, 75–93, doi:10.1007/s00382-008-0375-9.

Dewey, K. F., 1977: Daily Maximum and Minimum Temperature Forecasts and the Influence of Snow Cover. *Mon. Weather Rev.*, **105**, 1594-1597, doi:10.1175/1520-0493(1977)105<1594:DMAMTF>2.0.CO;2.

Dirmeyer, P. A., 2000: Using a Global Soil Wetness Dataset to Improve Seasonal Climate Simulation. *J. Clim.*, **13**, 2900-2922, doi:10.1175/1520-0442(2000)013<2900:UAGSWD>2.0.CO;2.

Dirmeyer, P. A., and Coauthors, 2016: Confronting Weather and Climate Models with Observational Data from Soil Moisture Networks over the United States. *Journal of Hydrometeorology*, **17**, 1049-1067, doi:10.1175/JHM-D-15-0196.1.

Domeisen, D. I. V., A. H. Butler, K. Fröhlich, M. Bittner, W. A. Müller, and J. Baehr, 2014: Seasonal Predictability over Europe Arising from El Niño and Stratospheric Variability in the MPI-ESM Seasonal Prediction System. *J. Clim.*, **28**, 256-271, doi:10.1175/JCLI-D-14-00207.1.

Douville, H., 2003: Assessing the influence of soil moisture on seasonal climate variability with AGCMs. *Journal of Hydrometeorology*, **4**, 1044-1066.

Douville, H., 2010: Relative contribution of soil moisture and snow mass to seasonal climate predictability: a pilot study. *Clim. Dyn.*, **34**, 797–818, doi:10.1007/s00382-008-0508-1.

Dunstone, N., D. Smith, A. Scaife, L. Hermanson, R. Eade, N. Robinson, M. Andrews, and J. Knight, 2016: Skilful predictions of the winter North Atlantic Oscillation one year ahead. *Nat. Geosci.*, **9**, 809–814, doi:10.1038/ngeo2824.

Dutra, E., C. Schär, P. Viterbo, and P. M. A. Miranda, 2011: Land-atmosphere coupling associated with snow cover. *Geophys. Res. Lett.*, **38**, L15707, doi:10.1029/2011GL048435.

Ebert-Uphoff, I. and Y. Deng, 2012: Causal Discovery for Climate Research Using Graphical Models. *J. Clim.*, **25**, 5648-5665, doi:10.1175/JCLI-D-11-00387.1.

Fletcher, C. G., S. C. Hardiman, P. J. Kushner, and J. Cohen, 2009: The Dynamical Response to Snow Cover Perturbations in a Large Ensemble of Atmospheric GCM Integrations. *J. Clim.*, **22**, 1208-1222.

Foster, J., M. Owe, and A. Rango, 1983: Snow Cover and Temperature Relationships in North America and Eurasia. *Journal of Climate and Applied Meteorology*, **22**, 460-469, doi:10.1175/1520-0450(1983)022<0460:SCATRI>2.0.CO;2.

Fritz, M. S. and D. P. MacKinnon, 2007: Required Sample Size to Detect the Mediated Effect. *Psychological science*, **18**, 233-239, doi:10.1111/j.1467-9280.2007.01882.x.

Jeong, J.-H., H. W. Linderholm, S.-H. Woo, C. Folland, B.-M. Kim, S.-J. Kim, and D. Chen, 2012: Impacts of Snow Initialization on Subseasonal Forecasts of Surface Air Temperature for the Cold Season. *J. Clim.*, **26**, 1956-1972, doi:10.1175/JCLI-D-12-00159.1.

Kolstad, E. W., E. A. Barnes, and S. P. Sobolowski, 2017: Quantifying the Role of Land–Atmosphere Feedbacks in Mediating Near-Surface Temperature Persistence. *Q. J. R. Meteorol. Soc.*, in press, doi:10.1002/qj.3033.

Koster, R. D., and Coauthors, 2011: The Second Phase of the Global Land–Atmosphere Coupling Experiment: Soil Moisture Contributions to Subseasonal Forecast Skill. *Journal of Hydrometeorology*, **12**, 805-822, doi:10.1175/2011JHM1365.1.

Koster, R. D., and Coauthors, 2010: Contribution of land surface initialization to subseasonal forecast skill: First results from a multi-model experiment. *Geophys. Res. Lett.*, **37**, L02402, doi:10.1029/2009GL041677.

Kretschmer, M., D. Coumou, J. F. Donges, and J. Runge, 2016: Using Causal Effect Networks to Analyze Different Arctic Drivers of Midlatitude Winter Circulation. *J. Clim.*, **29**, 4069-4081, doi:10.1175/JCLI-D-15-0654.1.

Kumar, S., and Coauthors, 2014: Effects of realistic land surface initializations on subseasonal to seasonal soil moisture and temperature predictability in North America and in changing climate simulated by CCSM4. *J. Geophys. Res. Atmos.*, **119**, 13,250-13,270, doi:10.1002/2014JD022110.

Leathers, D. J. and D. A. Robinson, 1993: The Association between Extremes in North American Snow Cover Extent and United States Temperatures. *J. Clim.*, **6**, 1345-1355, doi:10.1175/1520-0442(1993)006<1345:TABEIN>2.0.CO;2.

Lin, P., J. Wei, Z.-L. Yang, Y. Zhang, and K. Zhang, 2016: Snow data assimilation-constrained land initialization improves seasonal temperature prediction. *Geophys. Res. Lett.*, **43**, 11,423-11,432, doi:10.1002/2016GL070966.

MacKinnon, D. P., A. J. Fairchild, and M. S. Fritz, 2007: Mediation analysis. *Annu. Rev. Psychol.*, **58**, 593–614.

Matsumura, S. and K. Yamazaki, 2012: A longer climate memory carried by soil freeze–thaw processes in Siberia. *Environ. Res. Lett.*, **7**, 045402.

Mote, T. L., 2008: On the Role of Snow Cover in Depressing Air Temperature. *Journal of Applied Meteorology and Climatology*, **47**, 2008-2022, doi:10.1175/2007JAMC1823.1.

Namias, J., 1985: Some empirical evidence for the influence of snow cover on temperature and precipitation. *Mon. Weather Rev.*, **113**, 1542-1553.

Orsolini, Y., R. Senan, G. Balsamo, F. Doblas-Reyes, F. Vitart, A. Weisheimer, A. Carrasco, and R. Benestad, 2013: Impact of snow initialization on sub-seasonal forecasts. *Clim. Dyn.*, **41**, 1969-1982.

Orsolini, Y. J. and N. G. Kvamstø, 2009: Role of Eurasian snow cover in wintertime circulation: Decadal simulations forced with satellite observations. *J. Geophys. Res.*, **114**, D19108, doi:10.1029/2009jd012253.

Pearl, J., M. Glymour, and N. P. Jewell, 2016: *Causal Inference in Statistics: A Primer*. Wiley.

Peel, M., B. Finlayson, and T. McMahon, 2007: Updated world map of the Koppen-Geiger climate classification. *Hydrol. Earth Syst. Sci.*, **11**, 1633-1644.

Peings, Y., H. Douville, R. Alkama, and B. Decharme, 2011: Snow contribution to springtime atmospheric predictability over the second half of the twentieth century. *Clim. Dyn.*, **37**, 985–1004, doi:10.1007/s00382-010-0884-1.

Peings, Y., E. Brun, V. Mauvais, and H. Douville, 2013: How stationary is the relationship between Siberian snow and Arctic Oscillation over the 20th century? *Geophys. Res. Lett.*, **40**, 183-188, doi:10.1029/2012GL054083.

Poli, P., and Coauthors, 2016: ERA-20C: An Atmospheric Reanalysis of the Twentieth Century. *J. Clim.*, **29**, 4083-4097, doi:10.1175/JCLI-D-15-0556.1.

Potopová, V., C. Boroneanț, M. Možný, and J. Soukup, 2016: Driving role of snow cover on soil moisture and drought development during the growing season in the Czech Republic. *Int. J. Climatol.*, **36**, 3741-3758, doi:10.1002/joc.4588.

Prodhomme, C., F. Doblas-Reyes, O. Bellprat, and E. Dutra, 2016: Impact of land-surface initialization on sub-seasonal to seasonal forecasts over Europe. *Clim. Dyn.*, **47**, 919-935, doi:10.1007/s00382-015-2879-4.

Reichle, R. H., R. D. Koster, G. J. M. De Lannoy, B. A. Forman, Q. Liu, S. P. P. Mahanama, and A. Touré, 2011: Assessment and Enhancement of MERRA Land Surface Hydrology Estimates. *J. Clim.*, **24**, 6322-6338, doi:10.1175/JCLI-D-10-05033.1.

Reichle, R. H., C. S. Draper, Q. Liu, M. Girotto, S. P. P. Mahanama, R. D. Koster, and G. J. M. De Lannoy, 2017: Assessment of MERRA-2 Land Surface Hydrology Estimates. *J. Clim.*, **30**, 2937-2960, doi:10.1175/JCLI-D-16-0720.1.

Rienecker, M. M., and Coauthors, 2011: MERRA: NASA's modern-era retrospective analysis for research and applications. *J. Clim.*, **24**, 3624–3648.

Runge, J., V. Petoukhov, and J. Kurths, 2013: Quantifying the Strength and Delay of Climatic Interactions: The Ambiguities of Cross Correlation and a Novel Measure Based on Graphical Models. *J. Clim.*, **27**, 720-739, doi:10.1175/JCLI-D-13-00159.1.

Saha, S., and Coauthors, 2013: The NCEP Climate Forecast System Version 2. *J. Clim.*, **27**, 2185-2208, doi:10.1175/JCLI-D-12-00823.1.

Scaife, A. A., and Coauthors, 2014: Skillful long-range prediction of European and North American winters. *Geophys. Res. Lett.*, **41**, 2514–2519, doi:10.1002/2014GL059637.

Schlosser, C. A. and D. M. Mocko, 2003: Impact of snow conditions in spring dynamical seasonal predictions. *J. Geophys. Res. Atmos.*, **108**, 8616, doi:10.1029/2002JD003113.

Seneviratne, S. I., T. Corti, E. L. Davin, M. Hirschi, E. B. Jaeger, I. Lehner, B. Orlowsky, and A. J. Teuling, 2010: Investigating soil moisture–climate interactions in a changing climate: A review. *Earth-Science Reviews*, **99**, 125–161, doi:10.1016/j.earscirev.2010.02.004.

Shinoda, M., 2001: Climate memory of snow mass as soil moisture over central Eurasia. *J. Geophys. Res. Atmos.*, **106**, 33393-33403, doi:10.1029/2001JD000525.

Sobolowski, S., G. Gong, and M. Ting, 2010: Modeled climate state and dynamic responses to anomalous North American snow cover. *J. Clim.*, **23**, 785-799.

Thackeray, C. W. and C. G. Fletcher, 2016: Snow albedo feedback. *Progress in Physical Geography*, **40**, 392-408, doi:10.1177/0309133315620999.

Thomas, J. A., A. A. Berg, and W. J. Merryfield, 2016: Influence of snow and soil moisture initialization on sub-seasonal predictability and forecast skill in boreal spring. *Clim. Dyn.*, **47**, 49-65, doi:10.1007/s00382-015-2821-9.

van den Hurk, B., F. Doblas-Reyes, G. Balsamo, R. D. Koster, S. I. Seneviratne, and H. Camargo, 2012: Soil moisture effects on seasonal temperature and precipitation forecast scores in Europe. *Clim. Dyn.*, **38**, 349-362, doi:10.1007/s00382-010-0956-2.

Vavrus, S., 2007: The role of terrestrial snow cover in the climate system. *Clim. Dyn.*, **29**, 73-88.

Wagner, A. J., 1973: The Influence of Average Snow Depth on Monthly Mean Temperature Anomaly. *Mon. Weather Rev.*, **101**, 624-626, doi:10.1175/1520-0493(1973)101<0624:TIOASD>2.3.CO;2.

Walsh, J. E., D. R. Tucek, and M. R. Peterson, 1982: Seasonal Snow Cover and Short-Term Climatic Fluctuations over the United States. *Mon. Weather Rev.*, **110**, 1474-1486, doi:10.1175/1520-0493(1982)110<1474:SSCAST>2.0.CO;2.

Walsh, J. E., W. H. Jasperson, and B. Ross, 1985: Influences of Snow Cover and Soil Moisture on Monthly Air Temperature. *Mon. Weather Rev.*, **113**, 756-768, doi:10.1175/1520-0493(1985)113<0756:IOSCAS>2.0.CO;2.

Wegmann, M., Y. Orsolini, E. Dutra, O. Bulygina, A. Sterin, and S. Brönnimann, 2016: Eurasian snow depth in long-term climate reanalyses. *The Cryosphere Discuss.*, **2016**, 1-25, doi:10.5194/tc-2016-253.

Weisheimer, A., N. Schaller, C. O'Reilly, D. A. MacLeod, and T. Palmer, 2017: Atmospheric seasonal forecasts of the twentieth century: multi-decadal variability in predictive skill of the winter North Atlantic Oscillation (NAO) and their potential value for extreme event attribution. *Q. J. R. Meteorol. Soc.*, **143**, 917-926, doi:10.1002/qj.2976.

Yasunari, T., A. Kitoh, and T. Tokioka, 1991: Local and Remote Responses to Excessive Snow Mass over Eurasia Appearing in the Northern Spring and Summer Climate: A Study with the MRI GCM. *Journal of the Meteorological Society of Japan. Ser. II*, **69**, 473-487.

Zampieri, M., S. Russo, S. di Sabatino, M. Michetti, E. Scoccimarro, and S. Gualdi, 2016: Global assessment of heat wave magnitudes from 1901 to 2010 and implications for the river discharge of the Alps. *Science of The Total Environment*, **571**, 1330-1339, doi:10.1016/j.scitotenv.2016.07.008.

Zhang, T., 2005: Influence of the seasonal snow cover on the ground thermal regime: An overview. *Rev. Geophys.*, **43**, RG4002, doi:10.1029/2004RG000157.

Table

Table 1. Latitudes in degrees for the maximum zonal mean (denoted by overbars) values of τ and μ through Pathways A and B (denoted by subscripts). Greenland and ocean grid points were excluded when computing the zonal means, and a moving average spanning five latitude values was applied to the 'raw' zonal mean values.

Data set	ERA-20C			20CR		
Month pair	$\bar{\tau}$	$\bar{\mu}_A$	$\bar{\mu}_B$	$\bar{\tau}$	$\bar{\mu}_A$	$\bar{\mu}_B$
Feb/Mar	47	47	45	48.6	52.4	46.7
Mar/Apr	48	51	48	52.4	54.3	50.5
Apr/May	61	62	58	58.1	61.9	56.2
May/Jun	67	71	64	67.6	73.3	65.7

Preprints (www.preprints.org) | NOT PEER-REVIEWED | Posted: 3 May 2017 doi:10.20944/preprints201705.0029.v1

Figures

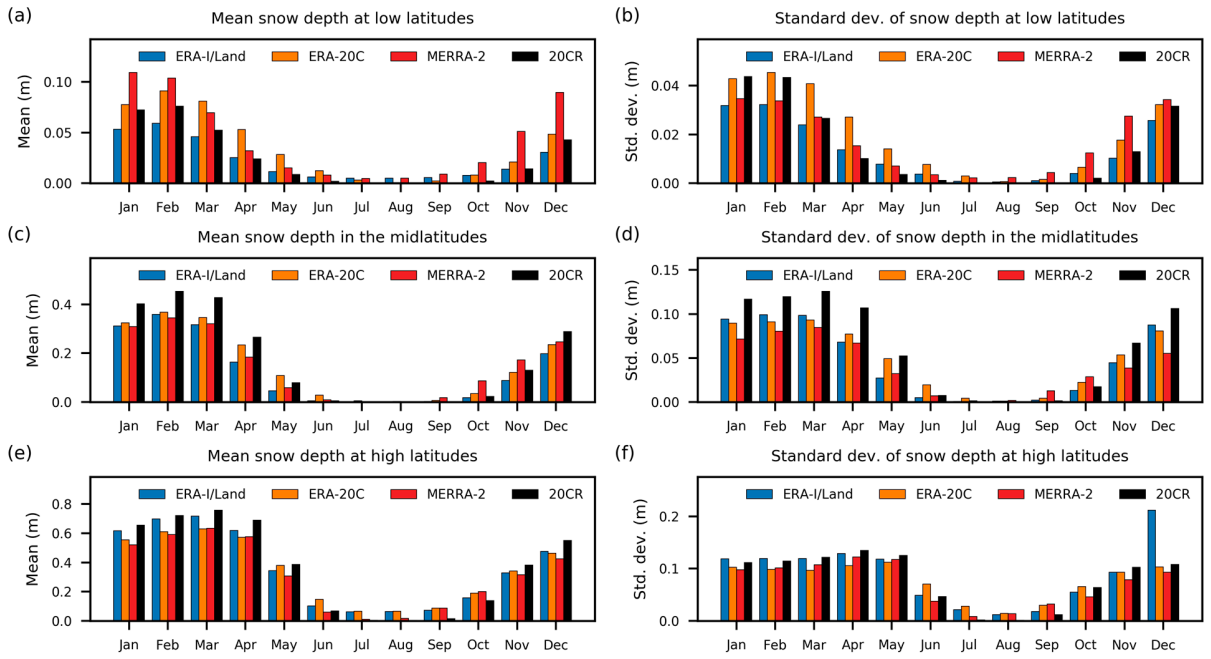

Fig. 1. Mean (a, c, and e) and standard devation (b, d, and f) of snow depth in 1980–2010 in meters, according to ERA-Interim/Land, MERRA-2, ERA-20C, and 20CR, as indicated. The values are area-averages in three latitude belts: (a–b) low latitudes (30°N–45°N), (c–d) midlatitudes (45°N–60°N), and (e–f) high latitudes (60°N–75°N, excluding Greenland).

Preprints (www.preprints.org) | NOT PEER-REVIEWED | Posted: 3 May 2017 doi:10.20944/preprints201705.0029.v1

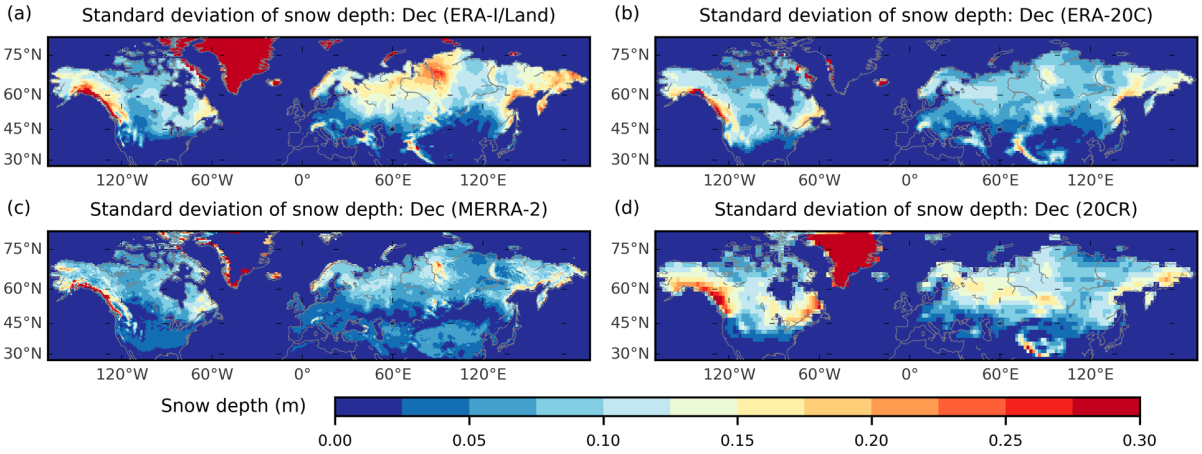

Fig. 2. Standard deviation of December (1980–2010) snow depth for ERA-Interim/Land (a), ERA-20C (b), MERRA-2 (c), and 20CR (d).

Preprints (www.preprints.org) | NOT PEER-REVIEWED | Posted: 3 May 2017 doi:10.20944/preprints201705.0029.v1

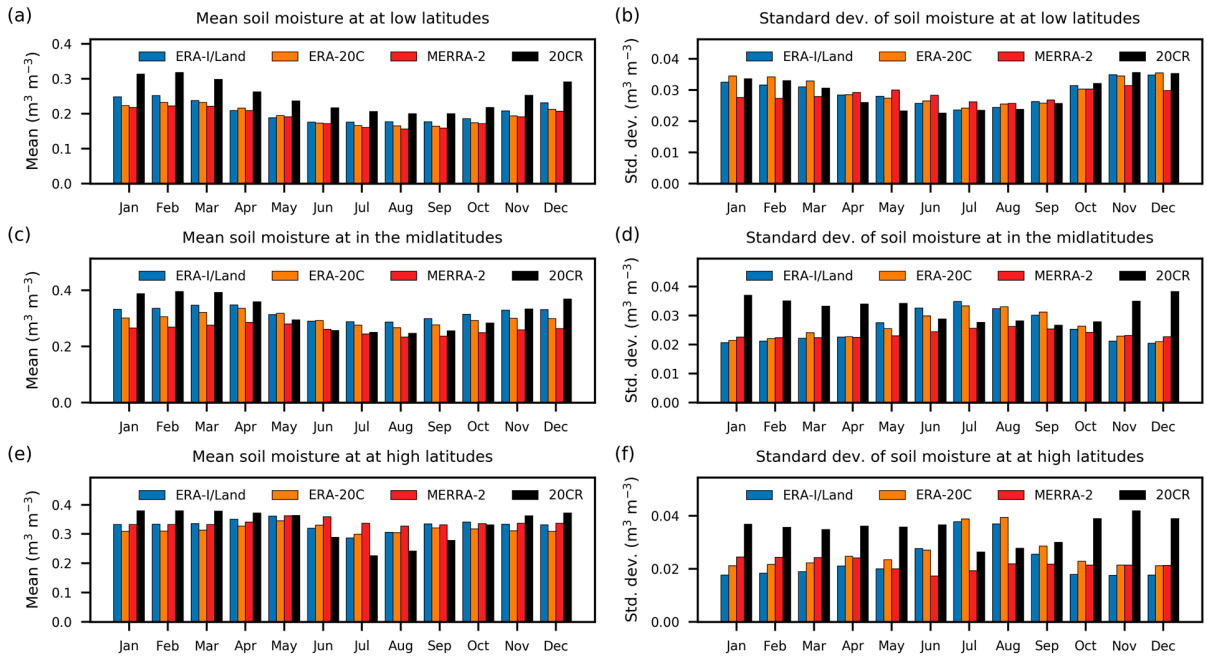

Fig. 3. As Fig. 1, but for soil moisture.

Preprints (www.preprints.org) | NOT PEER-REVIEWED | Posted: 3 May 2017 doi:10.20944/preprints201705.0029.v1

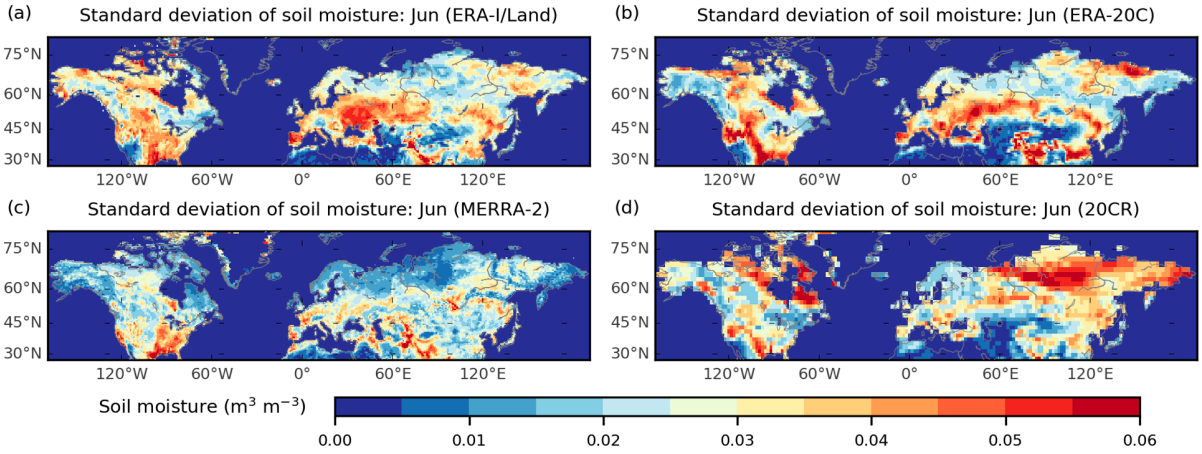

Fig. 4. Standard deviation of June (1980–2010) soil moisture for ERA-Interim/Land (a), ERA-20C (b), MERRA-2 (c), and 20CR (d).

Preprints (www.preprints.org) | NOT PEER-REVIEWED | Posted: 3 May 2017 doi:10.20944/preprints201705.0029.v1

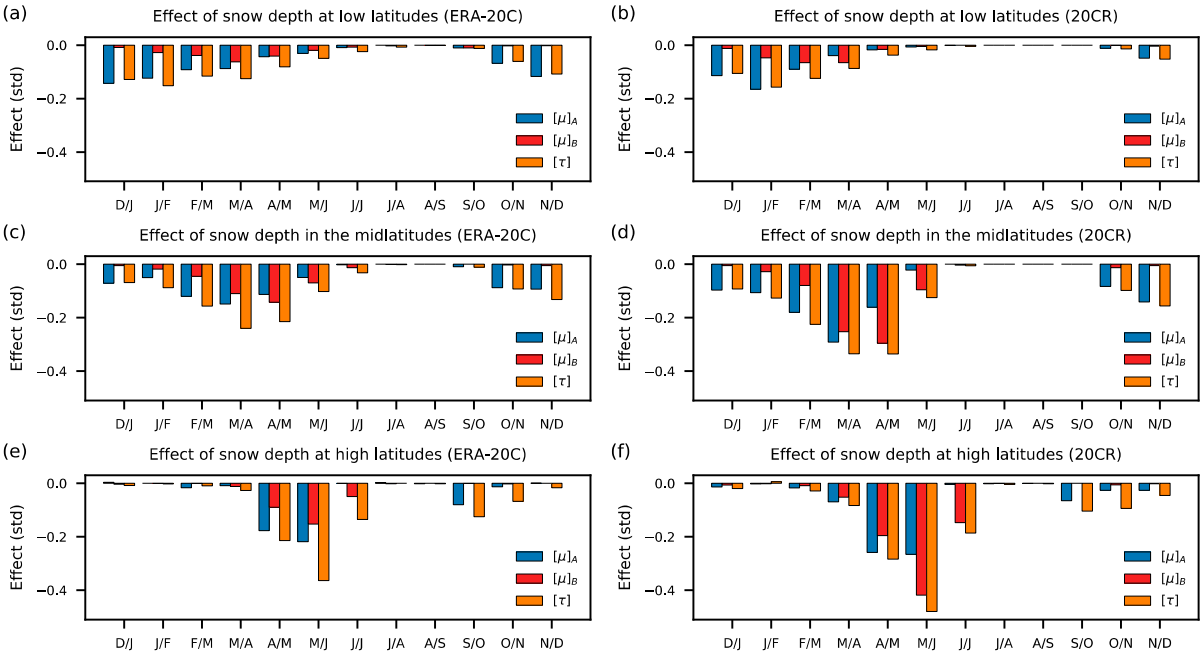

Fig. 5. In each panel, the total effect of snow depth on temperature (orange bars), and the mediated effects through partial mediation by snow depth (blue bars) and soil moisture (red bars) are shown, area-averaged in three latitude belts: (a–b) the low latitudes (30°N–45°N), (c–d) the midlatitudes (45°N–60°N, excluding Greenland), and (e–f) the high latitudes (60°N–75°N). The left column (a, c, and e) show results for ERA-20C, and the right column (b, d, and f) for 20CR.

Preprints (www.preprints.org) | NOT PEER-REVIEWED | Posted: 3 May 2017 doi:10.20944/preprints201705.0029.v1

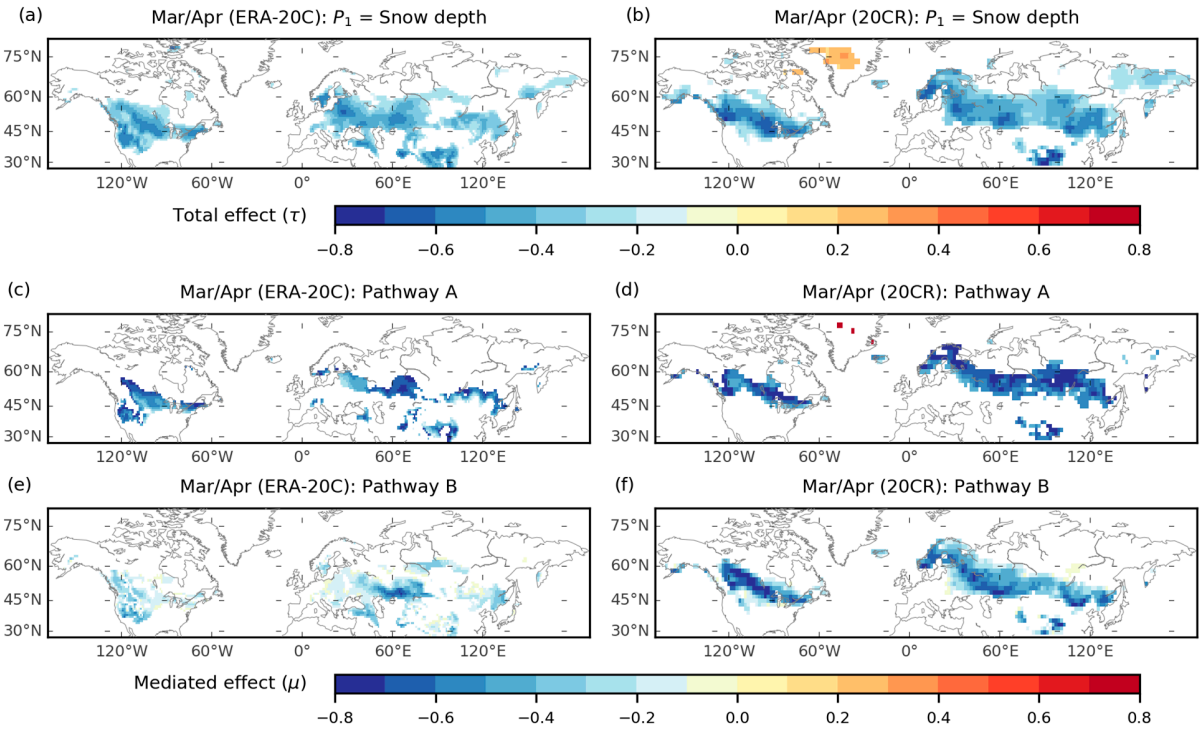

Fig. 6. (a–b) Lag-1 correlations between snow depth in March and temperature in April for the two reanalyses. The mediated effects of snow depth on temperature through Pathway A (c–d) and Pathway B (e–f) are also shown. Standardized time series are used. The left column (a, c, and e) show results for ERA-20C, and the right column (b, d, and f) for 20CR.

Preprints (www.preprints.org) | NOT PEER-REVIEWED | Posted: 3 May 2017 doi:10.20944/preprints201705.0029.v1

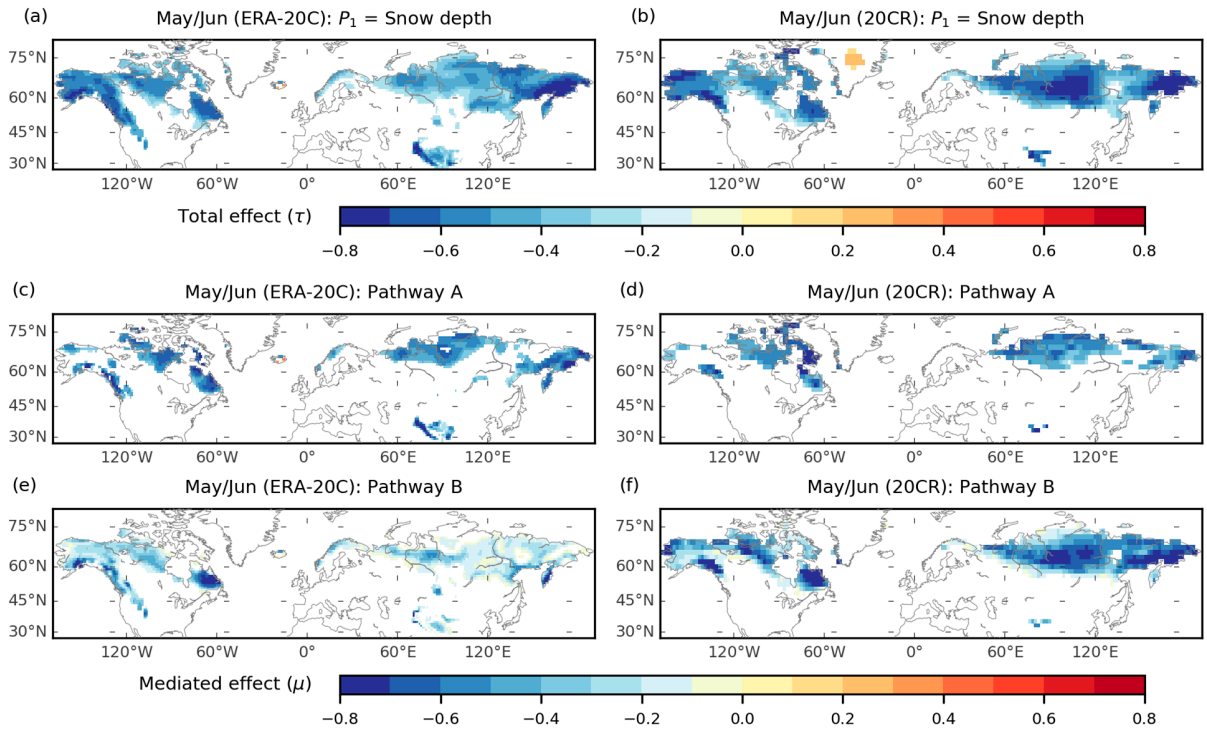

Fig. 7. As Fig. 6, but for May/June.